Supporting Information

Controlled co-reconstitution of multiple membrane proteins in lipid bilayer nanodiscs using DNA as a scaffold

Thomas Raschle[1,4,*], Chenxiang Lin[1,2,3], Ralf Jungmann[1,2,3], William M. Shih[1,2,3] & Gerhard Wagner[1,*]

[1] Department of Biological Chemistry and Molecular Pharmacology, Harvard Medical School, [2] Department of Cancer Biology, Dana-Farber Cancer Institute, and [3] Wyss Institute for Biologically Inspired Engineering, Harvard University, Boston, MA 02115, USA

* Corresponding authors: Gerhard Wagner and Thomas Raschle (e-mail: gerhard_wagner@hms.harvard.edu or traschle@creoptix.com)

[4] Current address: Einsiedlerstrasse 34, 8820 Wädenswil, Switzerland

ADDITIONAL EXPERIMENTAL PROCEDURES

Conjugation reaction – step 1: oligonucleotide-crosslinker. In a first step, the primary amine at the 5'-end of the oligonucleotide was reacted with the amine-reactive N-hydroxysuccinimide (NHS) ester moiety of the bifunctional crosslinker SM(PEG)$_4$. Briefly, HPLC-purified oligonucleotides with a free amine group at the 5'-end were purchased (Integrated DNA Technology). Oligonucleotides were dissolved in buffer C (50 mM NaPi, pH 7.5 and 150 mM NaCl) to give a final oligonucleotide concentration of 0.2 mM. The bifunctional crosslinker NHS-PEG$_4$-Maleimide (SM(PEG)$_4$; Thermo Scientific) was dissolved in anhydrous dimethylsulfoxide (DMSO) to give a final concentration of 250 mM. 25 nmoles of the oligonucleotide were incubated with a 50 times molar excess of crosslinker in 50 mM NaPi, pH 7.5, 150 mM NaCl, 0.2 mM EDTA and 10% DMSO for 30 min at 23°C. The reaction mix was applied to a disposable Sephadex G-25 column (illustra NAP-5; GE Healthcare) equilibrated in buffer C to remove excessive crosslinker. The oligonucleotide-crosslinker conjugate was precipitated by addition of 1/10 Vol. of 5 M NaCl and 3 Vol. of 100% (v/v) ice-cold ethanol. The reaction was incubated for 30 min at -30°C, centrifuged for 30 min at full speed at 4°C, washed with 4 Vol. ice-cold 75% (v/v) ethanol in water, centrifuged and the pellet dried for a few minutes in a speedvac.

Conjugation reaction – step 2: Protein-oligonucleotide. In a second step, the cysteine-reactive maleimide moiety of the oligonucleotide-crosslinker conjugate was reacted with the VDAC protein. Briefly, the oligonucleotide-crosslinker pellet was dissolved in buffer C and incubated with 0.5 mol equivalent of purified VDAC protein in 50 mM NaPi, pH 7.5 and 0.2 mM EDTA for 60 min at 35°C, followed by overnight incubation at 23°C.

Conjugation reaction – optional step: Protein-fluorophore: The VDAC protein was reacted overnight with 15 mol equivalent of an amine-reactive fluorescent dye (Alexa Fluor succinimidyl ester; Invitrogen) in 0.2 M sodium bicarbonate buffer, pH 8.3, at 23°C.

Purification of protein-oligonucleotide-fluorophore conjugate. The synthesized VDAC-oligonucleotide conjugates were purified by Ni-NTA affinity chromatography to remove excessive oligonucleotide-probe, followed by binding to an anion exchange column to separate unreacted VDAC protein from VDAC-oligonucleotide conjugate. As a final step, pooled fractions of the VDAC-oligonucleotide conjugate were purified by size exclusion chromatography and concentrated to approximately 10-20 µM with a yield of ~10% (relative to refolded VDAC protein). Briefly, the reaction was applied to a Ni-NTA column equilibrated in buffer D (5 mM imidazole, 50 mM NaPi, pH 8, 150 mM NaCl and 0.05% (w/v) LDAO) and washed with 10 column volumes of buffer D. The eluate in buffer E (200 mM imidazole, 50 mM NaPi, pH 8, 150 mM NaCl and 0.05% (w/v) LDAO) was diluted 1 to 1 with buffer F (20 mM Tris-Cl, pH 7.5, 0.2 mM EDTA, 0.1% (w/v) LDAO) and applied to a weak anion exchanger column (DEAE Ceramic HyperD F; Pall) in buffer F. The protein-oligonucleotide-fluorophore conjugate was eluted with a gradient of buffer G (1 M NaCl, 20 mM Tris-Cl, pH 7.5, 0.2 mM EDTA, 0.1% (w/v) LDAO). Protein containing fractions were pooled and exchanged into buffer H (20 mM Tris-Cl, pH 7.5, 250 mM NaCl, 0.2 mM EDTA and 0.1% (w/v) LDAO) on a size exclusion chromatography column (Superdex 200, 10/300; GE Healthcare). Fractions containing protein were pooled and concentrated in centrifugal filter units (Amicon Ultracel-10; Millipore). The concentration of protein and ratio of protein to fluorophore was estimated by measuring the absorbance at 260 nm (oligonucleotide), 280 nm, 495 nm (Alexa fluor 488), 578 nm (Alexa Fluor 568) and 650 nm (Alexa Fluor 647)

a

ID	Oligonucleotide sequence
t1	5' NH_2 - GTTGACGACGCCGTTTTTTCGTCTACTGCGCG
d2	5' NH_2 - CGCGCAGTAGACGTTTTTTCGGCGTCGTCAAC

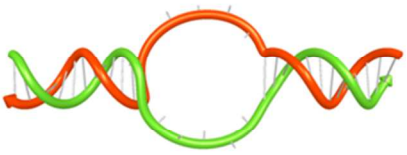

b

ID	Oligonucleotide sequence
t1	5' NH_2 - GTTGACGACGCCGTTTTTTCGTCTACTGCGCG
t2	5' NH_2 - CGCGCAGTAGACGTTTTTTCGACTCCCTACGC
t3	5' NH_2 - GCGTAGGGAGTCGTTTTTTCGGCGTCGTCAAC

Scheme S1. **Oligonucleotide building blocks and the duplex DNA scaffold structures.** Oligonucleotide sequences (top) used for the assembly of the duplex DNA scaffold (bottom) for dimeric (**a**) and trimeric (**b**) multimers. Complementary nucleotide sequences are either underlined with a solid or dotted line or printed in bold.

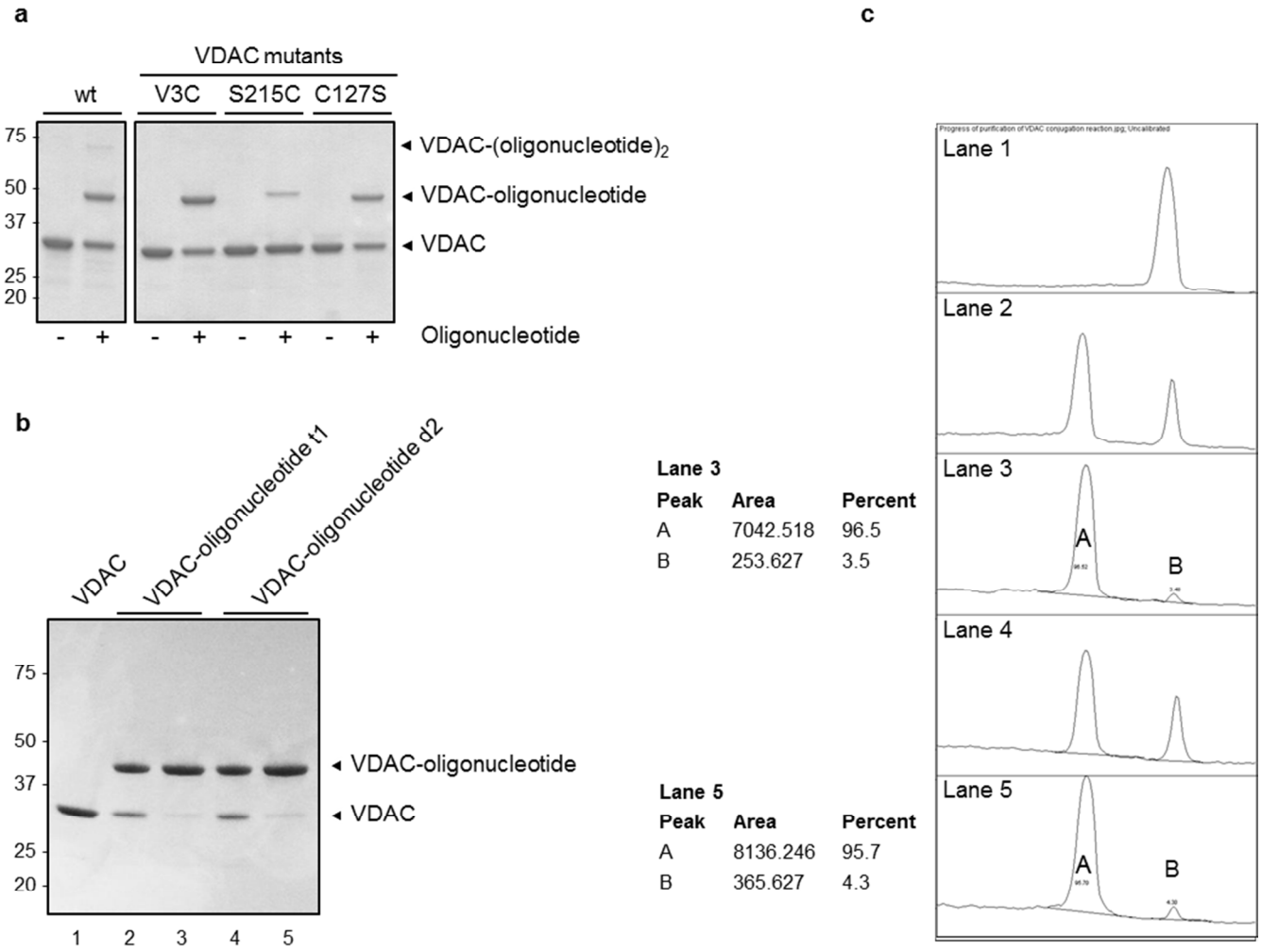

Figure S1. **Progress of the conjugation reaction of VDAC with oligonucleotide by SDS-PAGE.** (**a**) Different VDAC mutants were modified with the crosslinker probe and the yield of the reaction was monitored by SDS-PAGE. Shown are the following VDAC variants before and after modification with the oligonucleotide probe for 60 min at 35°C: wildtype (wt), V3C, S215C and C127S (resulting in the modification of C232). Note that the V3C- and S215C-VDAC mutants have a cysteine-less background, conferred by the C127S and C232S mutations. (**b**) SDS-PAGE analysis of the modification reaction of VDAC protein with oligonucleotide t1 (lane 2 and 3) and oligonucleotide d2 (lane 4 and 5) and subsequent purification. Lane 1, refolded and purified VDAC protein; lane 2 and 4, reaction product after conjugation with oligonucleotide t1 and d2, respectively; lane 3 and 5, t1 and d2 conjugation product after purification by Ni-NTA affinity chromatography, anion exchange chromatography and size exclusion chromatography. The purity of the VDAC-oligonucleotide conjugates was estimated to be ≥ 92%. (**c**) Estimation of the purity of the purified VDAC-oligonucleotide conjugates by SDS-PAGE. Shown are intensity plots of the 5 lanes from the gel shown in panel (b) and.

VDAC monomer	Mw (kDa)
VDAC	31.8

VDAC dimer	Mw (kDa)
VDAC-oligonucleotide-t1	42.3
VDAC-oligonucleotide-d2	42.3
VDAC-dimer	84.7

VDAC trimer	Mw (kDa)
VDAC-oligonucleotide-t1	42.3
VDAC-oligonucleotide-t2	42.3
VDAC-oligonucleotide-t3	42.4
VDAC-trimer	127.0

Table S1. **Molecular masses of the VDAC-conjugates and multimers used in this study.**

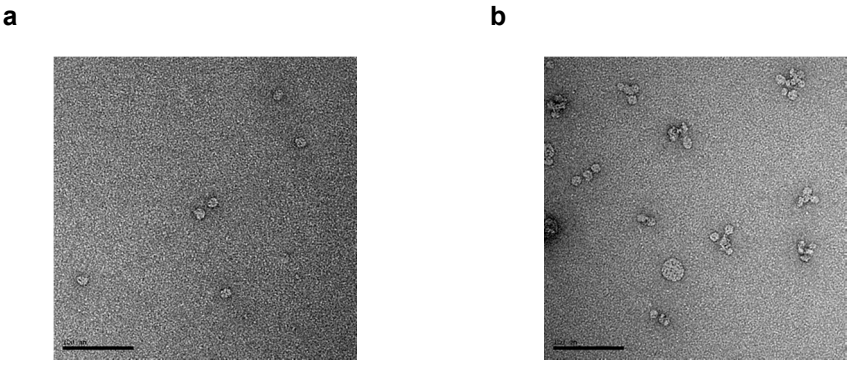

Figure S2. **Characterization of nanodiscs by negative stain transmission electron microscopy.** A representative image of the SEC peak fraction of (a) empty nanodiscs and (b) peak fraction C is shown. The scale bar is 100 nm.

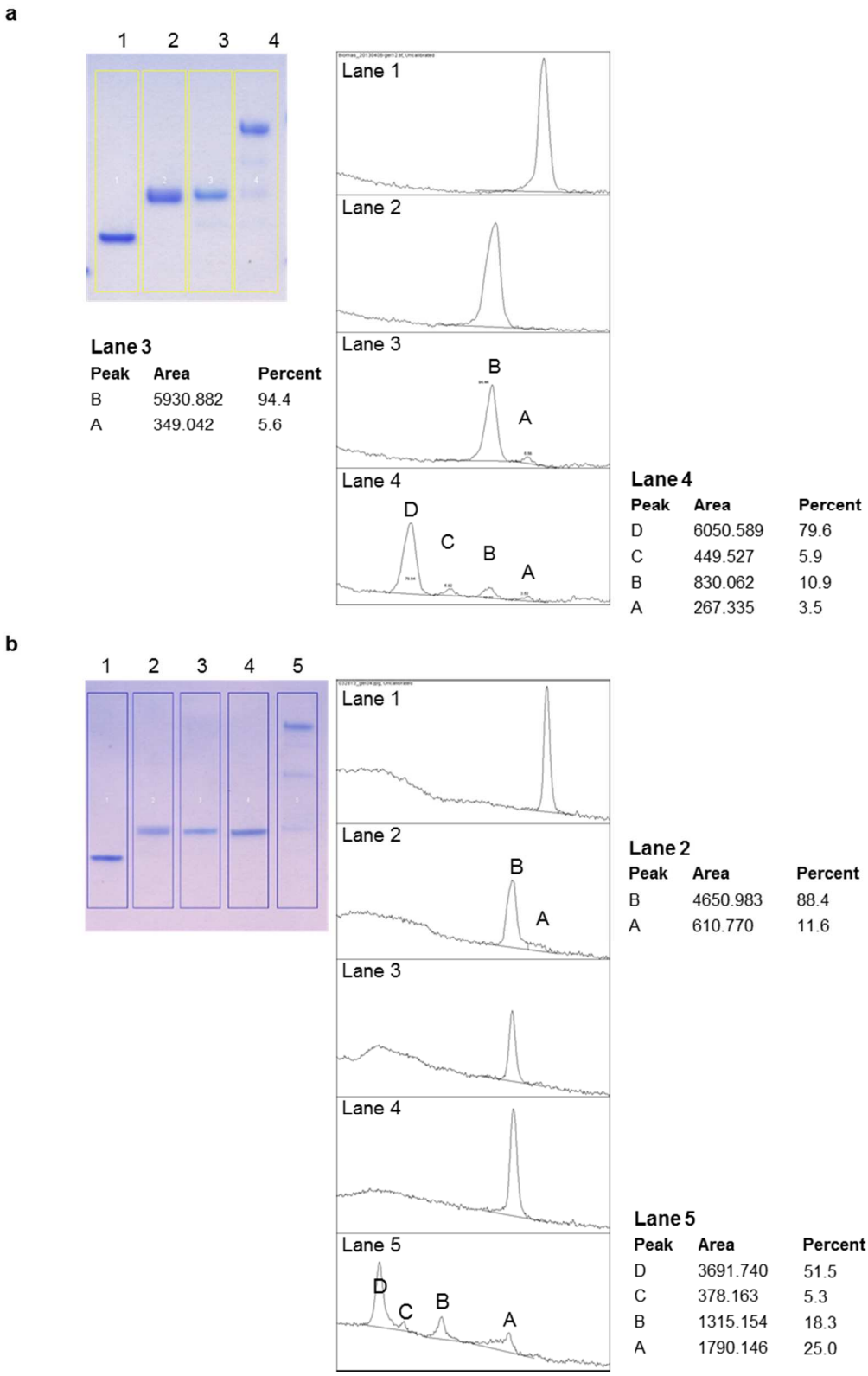

Figure S3. **Quantification of the purity of the purified VDAC-oligonucleotide conjugates and multimeric assemblies estimated by SDS-PAGE.** Shown are intensity plots for the gels shown in Figure 1a and 1b.

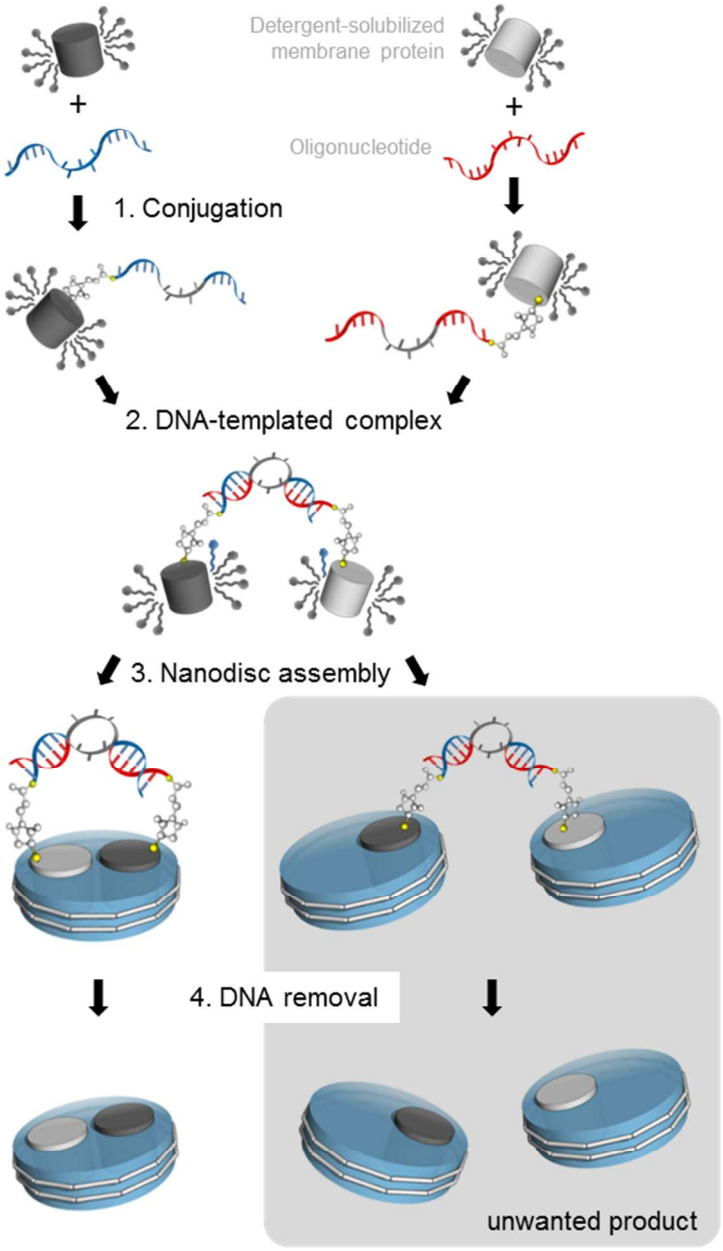

Scheme S2. **Tethering of two nanodiscs by the DNA scaffold.** The DNA scaffold facilitates the co-insertion of the tethered membrane proteins into a single nanodisc. However, the intrinsic flexibility of the described DNA scaffold can result in the insertion of the membrane proteins into separate nanodiscs, resulting in the tethering of two nanodiscs. Removal of the DNA linker results in the unwanted formation of nanodiscs containing only a single membrane protein.

$$P_{\text{co-localization}} = \frac{F_{VDAC-conjugate}}{2 - F_{VDAC-conjugate}}$$

Equation S1. $F_{VDAC\text{-}conjugate}$ is the fraction of VDAC-conjugate over total VDAC protein with the lowest labeling efficiency.

$$P_{dimer\ co-localization} = \left(\frac{c_{VDAC-conjugate\ 1}}{c_{nanodisc}}\right) \cdot \left(\frac{c_{VDAC-conjugate\ 2}}{c_{nanodisc}}\right)$$

Equation S2.

$$P_{trimer\ co-localization} = \left(\frac{c_{VDAC-conjugate\ 1}}{c_{nanodisc}}\right) \cdot \left(\frac{c_{VDAC-conjugate\ 2}}{c_{nanodisc}}\right) \cdot \left(\frac{c_{VDAC-conjugate\ 3}}{c_{nanodisc}}\right)$$

Equation S3.

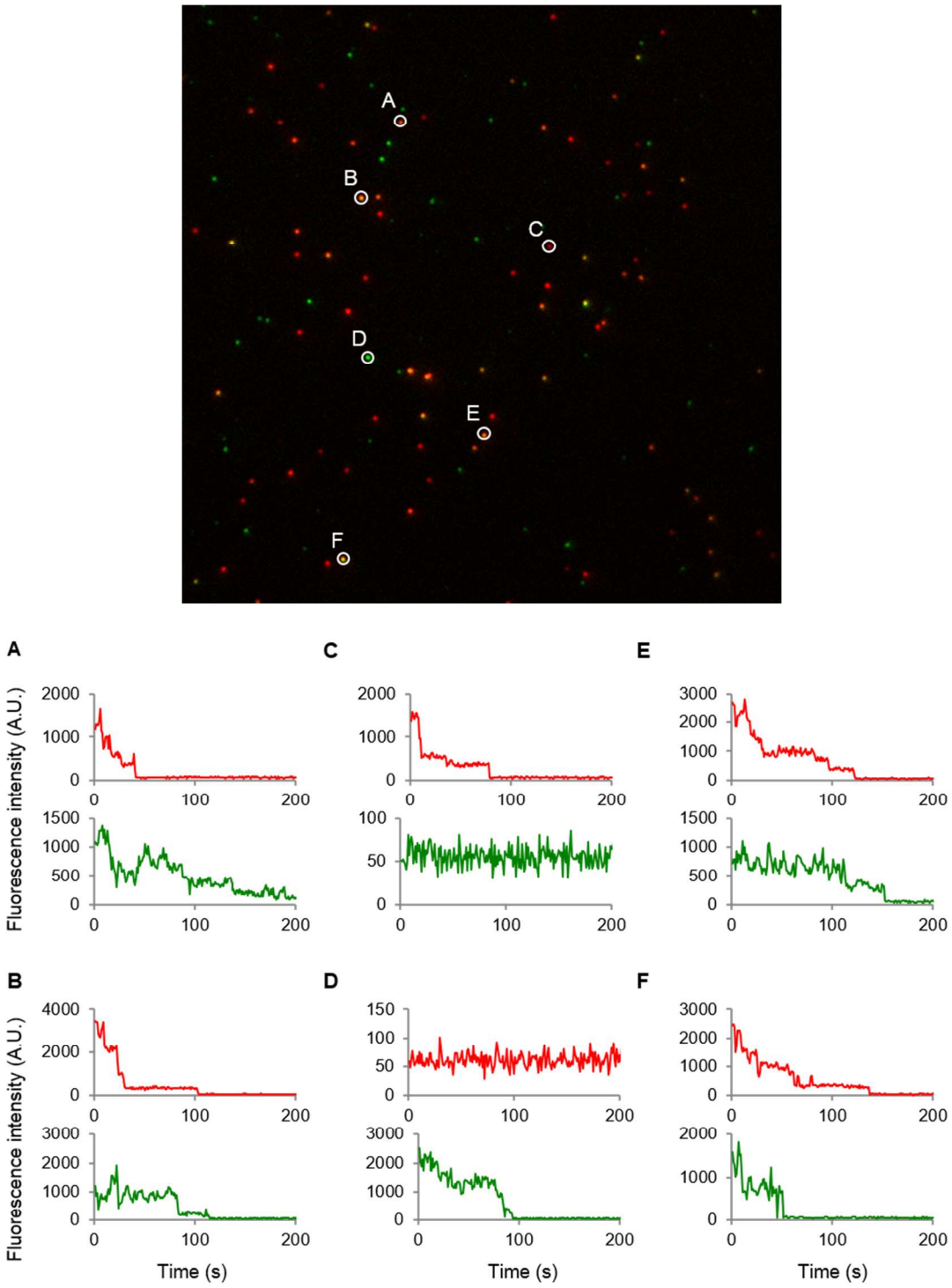

Figure S4. **Photobleaching analysis of $(VDAC)_2$-nanodiscs.** A TIRF image is shown at the top with six regions of interest marked. Integrated fluorescence intensity traces as a function of time are plotted at the bottom. The fluorescence emissions after excitation at 647 nm and 561 nm are shown as red and green traces, respectively. Stepwise photobleaching events indicate the attachment of multiple fluorescent dyes per VDAC protein. The observation of discrete photobleaching events for both fluorescence intensity traces indicates co-localization of the fluorescent dyes in single nanodiscs as shown for region A, B, E and F.

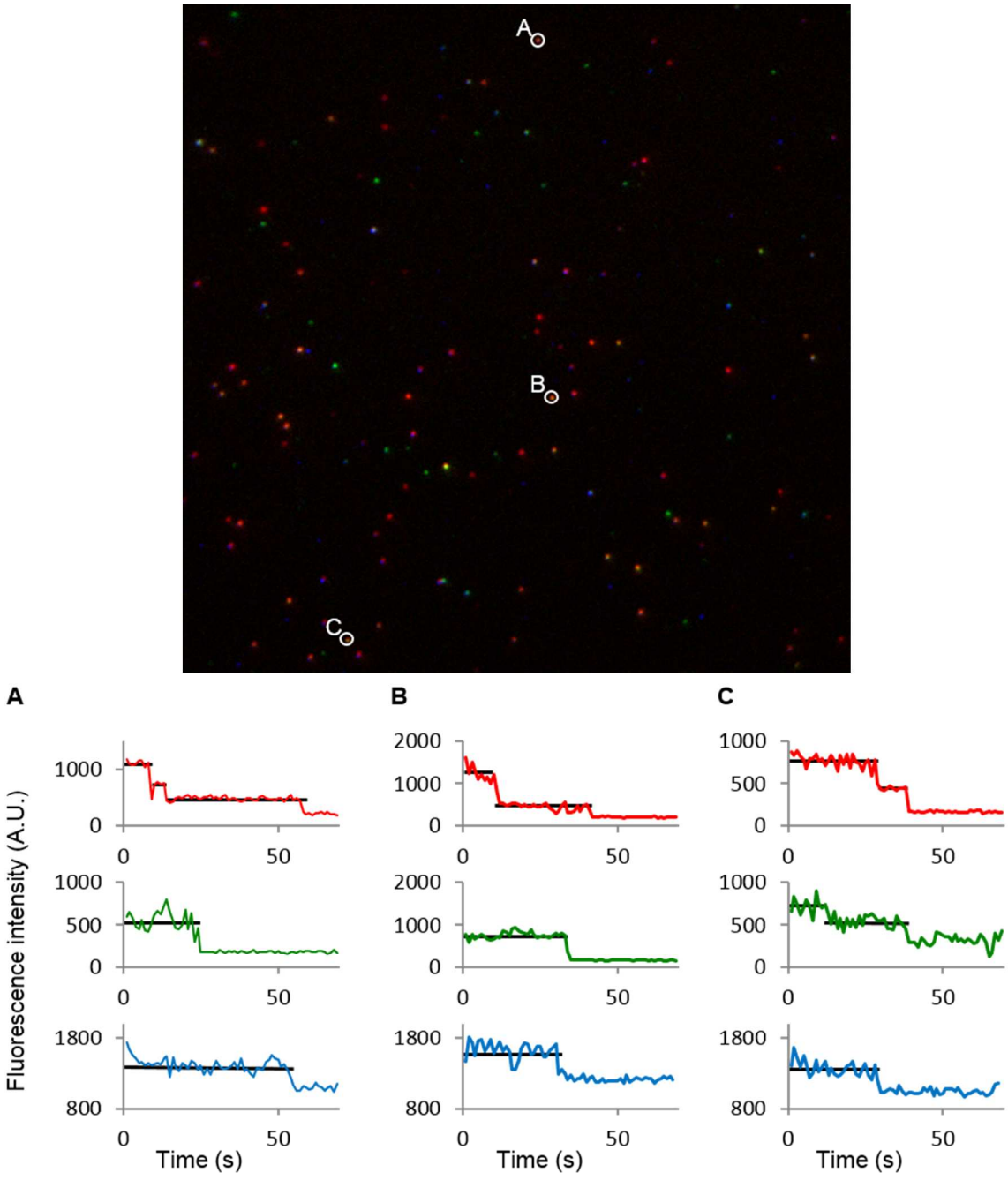

Figure S5. **Photobleaching analysis of $(VDAC)_3$-nanodiscs.** A TIRF image is shown at the top with three regions of interest marked. Integrated fluorescence intensity traces as a function of time are plotted at the bottom. The fluorescence emissions after excitation at 647 nm, 561 nm and 488 nm are shown as red, green and blue traces, respectively. Stepwise photobleaching events indicate the attachment of multiple fluorescent dyes per VDAC protein. The observation of discrete photobleaching events for all three fluorescence intensity traces indicates co-localization of the fluorescent dyes in single nanodiscs as shown for region A, B and C.

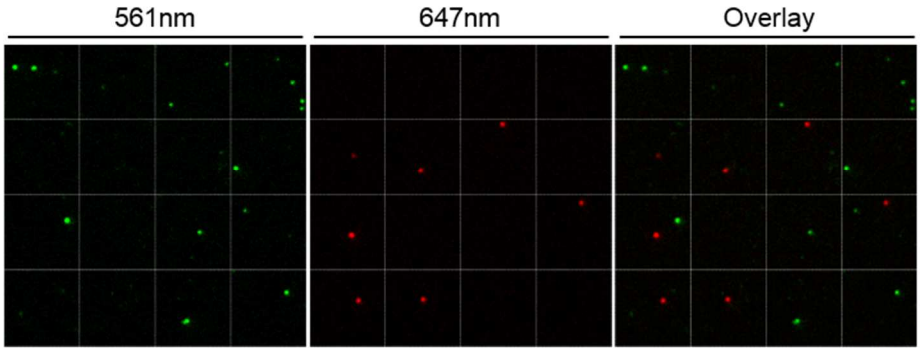

Figure S6. **Single molecule analysis of control nanodisc particles by fluorescence microscopy.** Representative TIRF image of nanodiscs assembled with un-tagged VDAC, i.e. in absence of a DNA scaffold. Note that two species of VDAC were used containing distinct fluorescent labels to mimic the assembly of heteromeric $(VDAC)_2$-nanodiscs in absence of the DNA-scaffold. Emitted fluorescent light was recorded from the same field of view after excitation at the wavelength specified. An overlay is shown on the right side. The images have dimensions of 27.3×27.3 μm.